

Beclin 1 deficiency is associated with increased hypoxia-induced angiogenesis

Seon-Jin Lee,¹ Hong Pyo Kim,² Yang Jin,¹ Augustine M.K. Choi¹ and Stefan W. Ryter^{1,*}

¹Division of Pulmonary and Critical Care Medicine; Brigham and Women's Hospital; Harvard Medical School; Boston, MA USA; ²School of Biological Sciences; College of Natural Sciences; University of Ulsan; Ulsan, Korea

Key words: angiogenesis, autophagy, beclin 1, hypoxia-inducible factor

Abbreviations: HIF, hypoxia-inducible factor; MLEC, mouse lung microvascular endothelial cells

Beclin 1, a tumor suppressor protein, acts as an initiator of autophagy in mammals. Heterozygous disruption of *Beclin 1* accelerates tumor growth, but the underlying mechanisms remain unclear. We examined the role of Beclin 1 in tumor proliferation and angiogenesis, using a primary mouse melanoma tumor model. *Beclin 1* (*Becn1*^{+/-}) hemizygous mice displayed an aggressive tumor growth phenotype with increased angiogenesis under hypoxia, associated with enhanced levels of circulating erythropoietin but not vascular endothelial growth factor, relative to wild-type mice. Using in vivo and ex vivo assays, we demonstrated increased angiogenic activity in *Becn1*^{+/-} mice relative to wild-type mice. Endothelial cells from *Becn1*^{+/-} mice displayed increased proliferation, migration and tube formation in response to hypoxia relative to wild-type cells. Moreover, *Becn1*^{+/-} cells subjected to hypoxia displayed increased hypoxia-inducible factor-2 α (HIF-2 α) expression relative to HIF-1 α . Genetic interference of HIF-2 α but not HIF-1 α , dramatically reduced hypoxia-inducible proliferation, migration and tube formation in *Becn1*^{+/-} endothelial cells. We demonstrated that mice deficient in the autophagic protein Beclin 1 display a pro-angiogenic phenotype associated with the upregulation of HIF-2 α and increased erythropoietin production. These results suggest a relationship between Beclin 1 and the regulation of angiogenesis, with implications in tumor growth and development.

Introduction

Angiogenesis, a multistep process involving cell proliferation, migration and maturation of neovessels, is required for tumor progression.¹ Rapidly growing tumors outpace the growth of their supporting vasculature and thereby lack oxygen and nutrients.²⁻⁴ Inadequate blood supply results in tissue hypoxia, a driving force behind the neovascularization of solid tumors. Adaptive responses to hypoxia are increasingly recognized as critical in physiological and pathological processes, and play important roles in tumor survival.^{5,6} Hypoxia induces the production of pro-angiogenic factors including vascular endothelial growth factor (VEGF)^{7,8} and erythropoietin (EPO).^{9,10}

Many cellular responses to hypoxia are regulated through the activation of hypoxia-inducible factor(s) (HIFs), which are heterodimers of the Per-Arnt-Sim (PAS)/basic helix-loop-helix family (bHLH) of transcription factors. HIF-1 consists of a constitutively expressed subunit (HIF-1 β), and an oxygen sensitive subunit (HIF-1 α). HIF-1 α is continuously degraded under normoxia by the proteasome, which is facilitated by the action of HIF prolyl hydroxylase and Von-Hippel Lindau E3: ubiquitin ligase. Recently a second oxygen-regulated subunit of HIF (HIF-2 α) also known as endothelial PAS domain protein 1 (EPAS1), has been implicated in the regulation of angiogenesis.^{11,12} Collectively,

HIFs regulate the expression of genes involved in energy metabolism, neovascularization, proliferation and cell migration, and thus act as promoters of tumor growth.^{13,14}

Autophagy, a homeostatic program for organelle or protein turnover and nutrient recycling, has recently been implicated as a physiological response to hypoxia.¹⁵ During this process, de novo synthesized double-membrane vesicles encapsulate cytosolic material, which is subsequently delivered to the lysosomes for proteolytic digestion.¹⁶ A number of genes critical for the regulation of autophagy (*Atg*) have been identified in mammals, each with distinct roles in the regulation of the autophagic pathway.¹⁷ Of these, Beclin 1, the mammalian homolog of yeast Atg6, plays a critical upstream regulatory function in the initiation of the autophagic pathway. Beclin 1 forms a multiprotein complex that includes class III phosphatidylinositol-3-kinase (PI3K) (*yeast*: Vps34) and p150 (*yeast*: Vps15). Additional proteins that can interact with this complex include the mammalian homolog of Atg14, the ultraviolet radiation resistance associated tumor suppressor gene protein (UVRAG) and Bcl-2 family proteins.¹⁸⁻²¹ Upon cellular stimulation, the increased production of phosphatidylinositol-3-phosphate by class III PI3K/Vps34 regulates the formation of nascent autophagosomes.²²

Beclin 1 is now recognized as a tumor suppressor protein, which inhibits cell growth and tumorigenesis.¹⁹

*Correspondence to: Stefan W. Ryter; Email: sryter@partners.org

Submitted: 10/15/10; Revised: 03/09/11; Accepted: 03/24/11

DOI: 10.4161/auto.78.15598

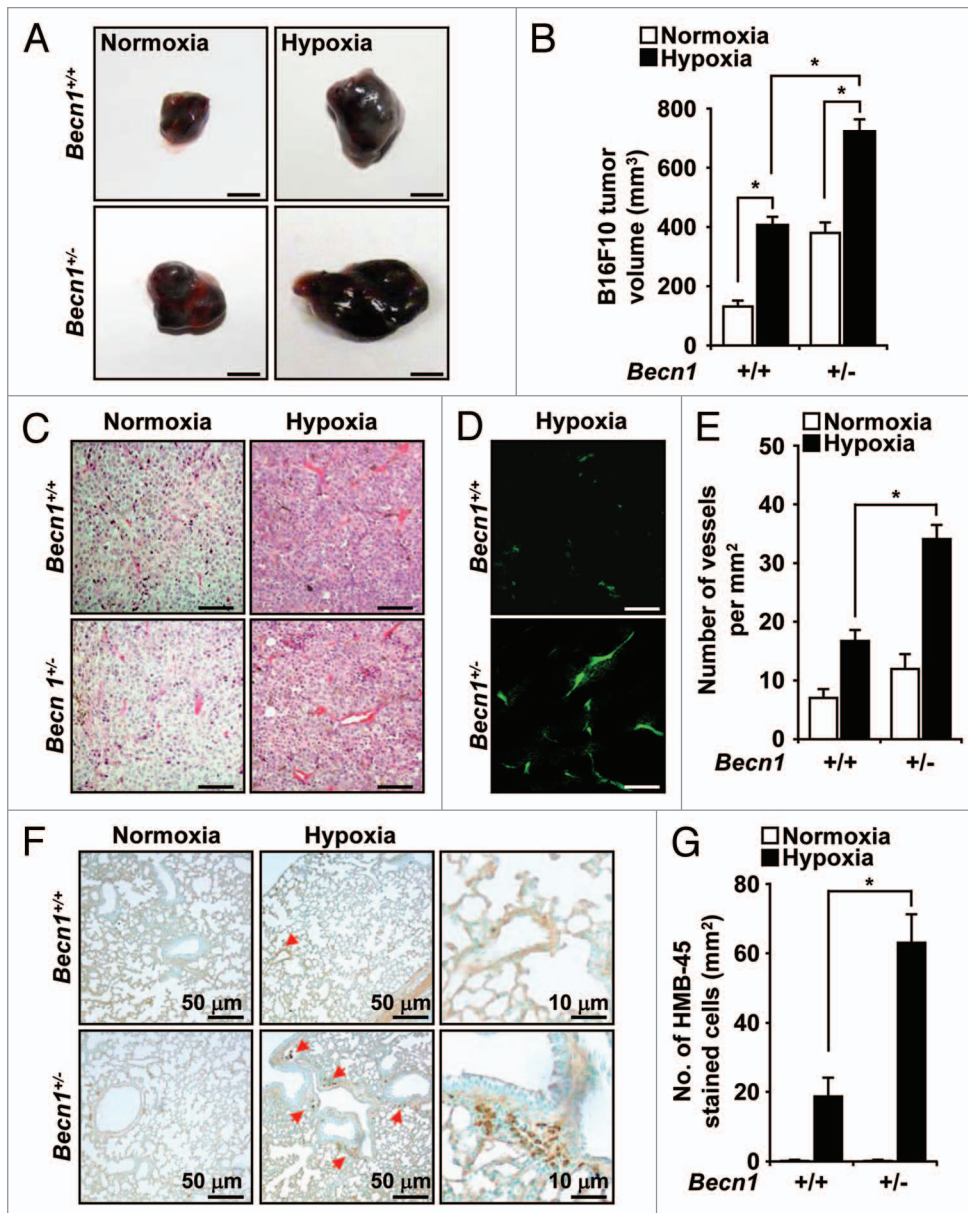


Figure 1. Heterozygous disruption of *Becn1* enhances hypoxia-induced tumor growth and angiogenesis. B16F10 melanoma cells were injected subcutaneously in *Becn1*^{+/+} and *Becn1*^{+/-} mice which were subsequently exposed to normoxia or hypoxia for 3 weeks. (A) Macroscopic appearance and (B) volume of B16F10 tumors from *Becn1*^{+/+} and *Becn1*^{+/-} mice after 3 weeks normoxia or hypoxia. Scale bar, 5 mm. The graph shows mean tumor volume \pm SD, (**p* < 0.05, Student's *t*-test), *n* = 7 mice per treatment group. (C) H&E and (D) CD31 staining of B16F10 tumor sections from *Becn1*^{+/+} or *Becn1*^{+/-} mice exposed to hypoxia for 3 weeks. Scale bars, 10 μ m. (E) Blood vessel density in tumors from *Becn1*^{+/+} or *Becn1*^{+/-} mice. Vessel density was quantified by counting the number of vessels per mm² in CD31 stained sections. Data represent the mean \pm SD, *n* = 5–6 tumors per group (**p* < 0.05, Student's *t*-test). (F) HMB45 staining of melanoma cells in lung sections from tumor-bearing mice after 3 weeks of hypoxia exposure. Red arrows indicate HMB45 positive cells. Scale bars, 50 μ m (left part) and 10 μ m (right part). (G) Quantification of HMB45 stained cells in lung tissues from B16F10-injected *Becn1*^{+/+} and *Becn1*^{+/-} mice exposed to normoxia or hypoxia for 3 weeks. Data represent mean \pm SD. (**p* < 0.05, Student's *t*-test), *n* = 5–6 lungs per condition.

Becn1 heterozygous knockout mice (*Becn1*^{+/-}) display increased tumor formation in vivo.^{18,19} However, the specific mechanism by which Beclin 1 serves as a tumor suppressor molecule is not known.

In the current study we show increases in tumor growth and angiogenesis of implanted melanoma tumors in *Becn1*^{+/-} mice relative to their wild-type counterparts. These phenotypic observations in *Becn1*^{+/-} mice were accompanied by differential expression of HIF-2 α and increased levels of circulating erythropoietin (EPO). A better understanding of how autophagic proteins can regulate the angiogenic process may lead to novel therapeutic strategies in the treatment of cancer or vascular disorders.

Results

Becn1^{+/-} mice display enhanced growth, angiogenesis and migration of implanted melanoma tumors. To examine the

underlying mechanism(s) by which Beclin 1 inhibits tumorigenesis, we monitored the primary growth of a B16F10 melanoma tumor cell line implanted subcutaneously in *Becn1* hemizygous knockout (*Becn1*^{+/-}) mice or their corresponding wild-type (*Becn1*^{+/+}) littermate mice. In wild-type mice, hypoxia exposure (3 weeks) enhanced tumor growth relative to normoxia (Fig. 1A). In contrast, tumor size and volume were dramatically increased in *Becn1*^{+/-} mice relative to *Becn1*^{+/+} mice under hypoxic conditions (Fig. 1A and B). A modest increase in tumor size was also observed in *Becn1*^{+/-} mice relative to *Becn1*^{+/+} mice under normoxic conditions (Fig. 1A and B).

To examine whether differential tumor angiogenesis can account for these findings, we isolated B16F10 tumor tissue sections from *Becn1*^{+/-} or *Becn1*^{+/+} mice after 3 weeks of hypoxia exposure. Significant increases in vascularization were observed in tumor tissue recovered from *Becn1*^{+/-} mice relative to *Becn1*^{+/+} mice by hematoxylin and eosin (Fig. 1C) and immunofluorescence staining using an antibody against CD31 (platelet endothelial cell adhesion molecule-1), a marker of endothelial cells (Fig. 1D and E). No significant differences in tumor vascularization were observed between the strains under normoxic conditions.

To evaluate the occurrence and proliferation of melanoma cells in the lungs of tumor-bearing mice, we stained lung tissue sections from *Becn1^{+/-}* or *Becn1^{+/+}* mice for the melanoma-specific marker HMB45 (Fig. 1F and G). The abundance of HMB45-positive cells was greater in the lungs of *Becn1^{+/-}* mice relative to *Becn1^{+/+}* mice after 3 weeks of hypoxia. No significant differences were observed between the strains under normoxic conditions.

***Becn1^{+/-}* mice display enhanced erythropoietin production during hypoxia.** Hypoxia can stimulate the release of growth factors such as VEGF and EPO which stimulate vascular cell proliferation and angiogenesis.⁷⁻¹⁰ While circulating EPO levels were increased in the plasma after hypoxic exposure, the production of EPO was markedly elevated in the *Becn1^{+/-}* relative to *Becn1^{+/+}* mice (Fig. 2A). In contrast, no differences in the circulating levels of VEGF were detected between the strains (Fig. 2B). Similar results were observed in tumor bearing *Becn1^{+/-}* or *Becn1^{+/+}* mice exposed to hypoxia (Fig. 2C and D).

***Becn1^{+/-}* mice are compromised for hypoxia-inducible autophagy.** The *Becn1^{+/-}* mice were analyzed for Beclin 1 phenotype and activation of autophagy in the lung in response to hypoxia. Beclin 1 expression was moderately increased by hypoxia in wild-type mice. In contrast, the *Becn1^{+/-}* mice displayed decreased expression of Beclin 1 in the lung under basal conditions, as well as after hypoxia stimulation, relative to *Becn1^{+/+}* mice (Fig. 3A). Interestingly, *Becn1^{+/-}* mice also displayed reduced expression and activation of the autophagic protein LC3B, as indicated by decreased accumulation of LC3B-I and its faster migrating, lipid-conjugated active form LC3B-II, under both normoxic and hypoxic conditions, relative to wild-type mice (Fig. 3A). Autophagosome formation was increased in the lung tissue of hypoxia exposed wild-type animals. In contrast, *Becn1^{+/-}* mice had markedly reduced autophagosome formation in lung tissue relative to wild-type mice (Fig. 3B).

***Becn1^{+/-}* vascular cells display enhanced proliferation, migration and tube formation in vitro.** We examined whether Beclin 1 can influence the angiogenic activity of endothelial cells. Mouse lung endothelial cells (mLEC) isolated from *Becn1^{+/-}* or *Becn1^{+/+}* mice were cultured under normoxia or hypoxia and assayed for proliferation. Under normoxic conditions, there was no apparent difference in cellular proliferation between *Becn1^{+/-}* mLEC and *Becn1^{+/+}* mLEC (Fig. 4A). The *Becn1^{+/-}* mLEC exhibited greater proliferation under hypoxia than the *Becn1^{+/+}* mLEC (Fig. 4B and C). We also evaluated the role of Beclin 1 in pulmonary vascular cell proliferation. Stimulation with endothelin-1 (ET-1, 40 nM) or PDGF-BB (20 ng ml⁻¹) for 48 hrs during hypoxia increased cell proliferation in PAEC (Fig. 4D) and PSMC (Fig. 4E), respectively. Infection with *Becn1*-specific siRNA further increased hypoxia and mitogen-dependent cell

Figure 3. Decreased autophagy phenotype in *Becn1^{+/-}* mice. The *Becn1^{+/+}* and *Becn1^{+/-}* mouse were exposed to hypoxia or normoxia for 3 weeks. (A) Lung tissue homogenates were analyzed for the expression of LC3B-I/II and Beclin 1 by western immunoblot analysis. β -actin served as the standard. (B) Lung tissue sections were fixed in glutaraldehyde and analyzed by electron microscopy for immature (AVI) or degradative (AVd) autophagosome formation. Total autophagosome formation per 100 μ m² area is quantitated from N = 15 sections.

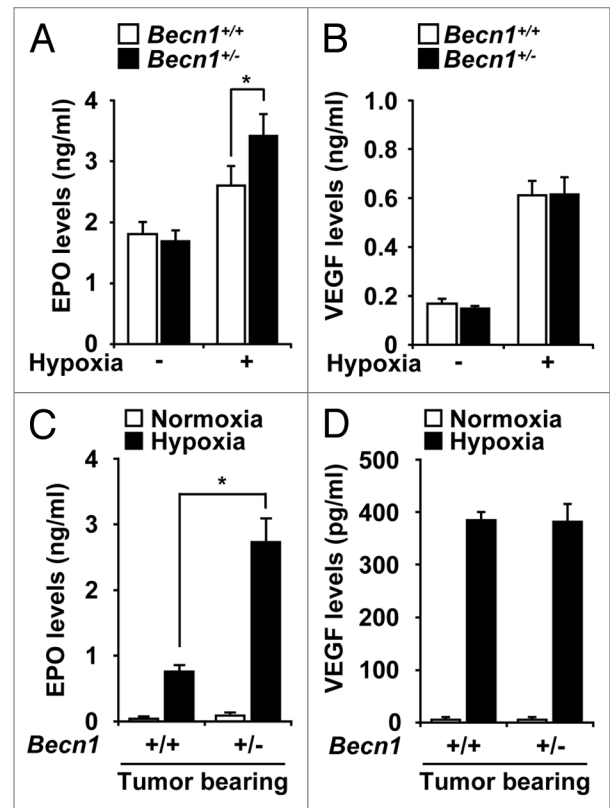
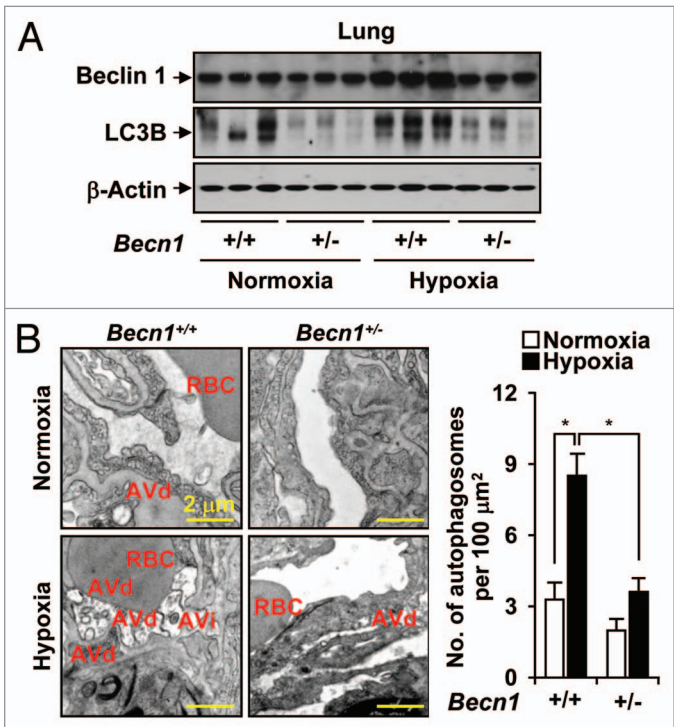


Figure 2. Beclin 1 deficiency results in enhanced levels of EPO production during hypoxia exposure in mice. Quantification of (A) VEGF and (B) EPO production in *Becn1^{+/+}* and *Becn1^{+/-}* mouse plasma was determined by Quantikine™ ELISA after hypoxia exposure for 3 weeks. Data are means \pm SEM. (* $p < 0.05$, Student's t-test), ($n = 10$ per group). (C and D) Circulating levels of VEGF and EPO from the plasma of B16F10-injected mice exposed to hypoxia for 3 weeks. (* $p < 0.05$, Student's t-test), ($n = 7$ per group).



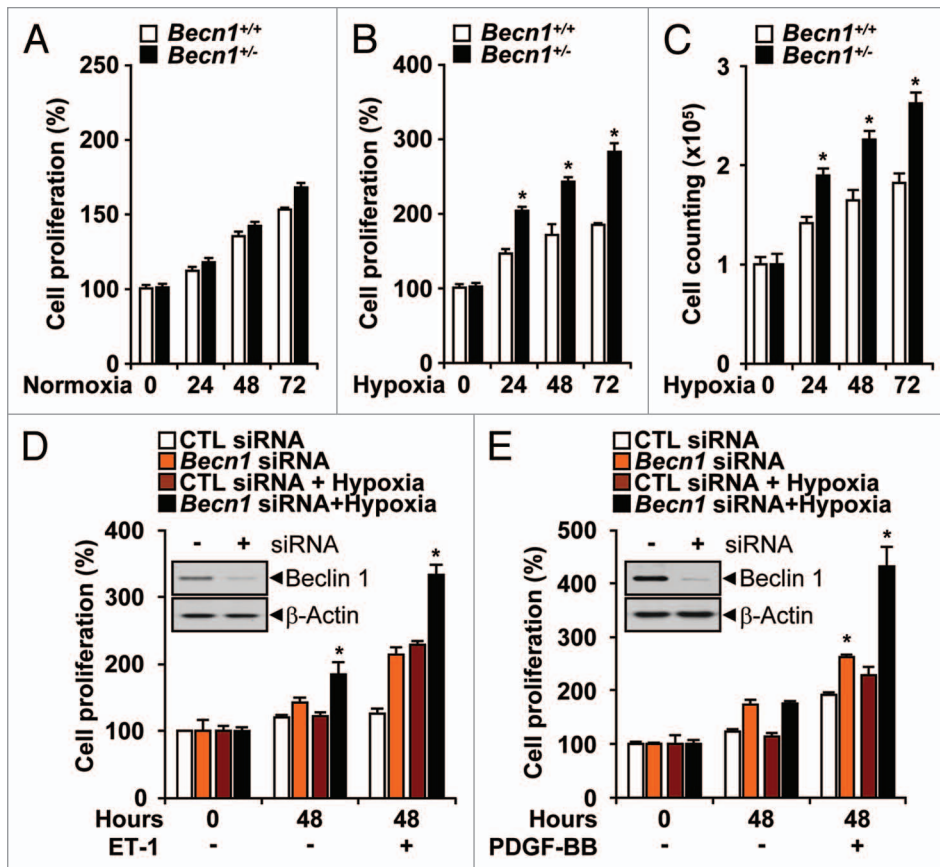


Figure 4. Heterozygous disruption of *Becn1* promotes hypoxia-induced endothelial cell proliferation, migration and tube formation. (A) The proliferation of *Becn1*^{+/+} and *Becn1*^{+/-} mLECs exposed to normoxia was assessed by crystal violet staining. (B and C) Proliferation indices of mLECs exposed to hypoxia (1% O₂) were assessed by crystal violet and Trypan blue exclusion methods. Data represent means ± SEM from experiments in triplicate (*p < 0.05, Student's t-test). (D and E) PAECs or PASCs were transfected with control or *Becn1* siRNA. Western (inserts) shows validation of Beclin 1 expression levels following control or *Becn1* siRNA treatment. β-actin served as the standard. (D) Following addition of ET-1 (40 nM), PAEC cultures were exposed to hypoxia or normoxia for an additional 48 h. Data represent means ± SEM in triplicate experiments. (*p < 0.05, Student's t-test). (E) Following addition of PDGF-BB (20 ng/ml) siRNA transfected PASC cultures were exposed to hypoxia or normoxia for an additional 48 h. Data represent means ± SEM from three independent experiments. (*p < 0.05, Student's t-test).

proliferation relative to control siRNA-infected cells (Fig. 4D and E). Furthermore, *Becn1*^{+/-} mLECs displayed enhanced hypoxia-induced cell migration relative to *Becn1*^{+/+} mLECs (Fig. 5A and B). The function of Beclin 1 in the morphological differentiation of mLECs was investigated using a two-dimensional Matrigel assay. When plated on growth factor-reduced Matrigel, *Becn1*^{+/+} mLEC formed an incomplete tube network under normoxic conditions relative to *Becn1*^{+/-} mLEC. Hypoxia exposure stimulated extensive tube networks in *Becn1*^{+/-} mLECs, and a greater number of cell connections relative to *Becn1*^{+/+} mLECs (Fig. 5C and D).

***Becn1*^{+/-} mice display enhanced angiogenesis in vivo.** We investigated whether Beclin 1 regulates neovascularization in vivo by injecting Matrigel as subcutaneous plugs into *Becn1*^{+/+} and *Becn1*^{+/-} mice (Fig. 6A). Significant blood vessel formation and inflammatory infiltrate were apparent in cross-sections of Matrigel plugs recovered from both normoxia and hypoxia treated mice 14

days after implantation, indicating the existence of a functional vasculature within these plugs. The Matrigel plugs were stained with anti-CD31 antibody for analysis of vessel density (Fig. 6B). The CD31 positive staining demonstrated a greater density of functional vasculature in the plugs recovered from *Becn1*^{+/-} mice relative to *Becn1*^{+/+} mice (Fig. 6C). To confirm the role of Beclin 1 in anti-angiogenesis, we cultured mouse aortic ring explants under normoxia and hypoxia (Fig. 6D). Exposure to hypoxia resulted in an approximate three-fold increase in vessel sprouting at the severed edge of mouse aortic rings derived from *Becn1*^{+/-} mice relative to those from *Becn1*^{+/+} mice (Fig. 6E).

Enhanced stress-response in *Becn1*^{+/-} endothelial cells. Previous studies have suggested that autophagy deficiency in mice can promote oxidative stress, inflammation and increased pro-inflammatory cytokine production.²³⁻²⁶ We examined whether endothelial cells derived from *Becn1*^{+/-} mice display altered regulation of stress response or pro-inflammatory mediators. Cultured *Becn1*^{+/-} mLEC displayed increased expression of Nrf-2, a master regulator of stress-gene expression, under normoxic or hypoxic conditions, relative to wild-type mLEC (Fig. 7A). Conversely, the expression levels of Keap-1, the cytoplasmic anchor of Nrf-2, were reduced in *Becn1*^{+/-} mice under normoxic or hypoxic conditions, relative to wild-type mLEC (Fig. 7A). Furthermore, *Becn1*^{+/-} mLEC displayed increased levels of the phospho-form of the p65 subunit of NFκB, a master regulator of inflammatory responses, under normoxic or hypoxic conditions, relative to wild-type mLEC (Fig. 7B).

Enhanced expression and stability of hypoxia-inducible HIF-2α protein in *Becn1*^{+/-} endothelial cells. Since HIFs are critical regulators of hypoxia-dependent gene expression,^{27,28} we examined the kinetics of HIF-1α and HIF-2α expression in response to hypoxia in tumors and vascular cells derived from *Becn1*^{+/-} or *Becn1*^{+/+} mice.

In tumor tissue recovered from *Becn1*^{+/-} or *Becn1*^{+/+} mice, there was no apparent difference in HIF-1α or HIF-2α expression between the strains (Fig. 8A). In mLEC isolated from *Becn1*^{+/+} mice, hypoxia (1% O₂) time-dependently increased HIF-1α but not HIF-2α expression (Fig. 8B). In contrast, hypoxia increased the level of HIF-2α relative to HIF-1α in *Becn1*^{+/-} mLEC. This preferential activation of HIF-2α in *Becn1*^{+/-} mLEC was also

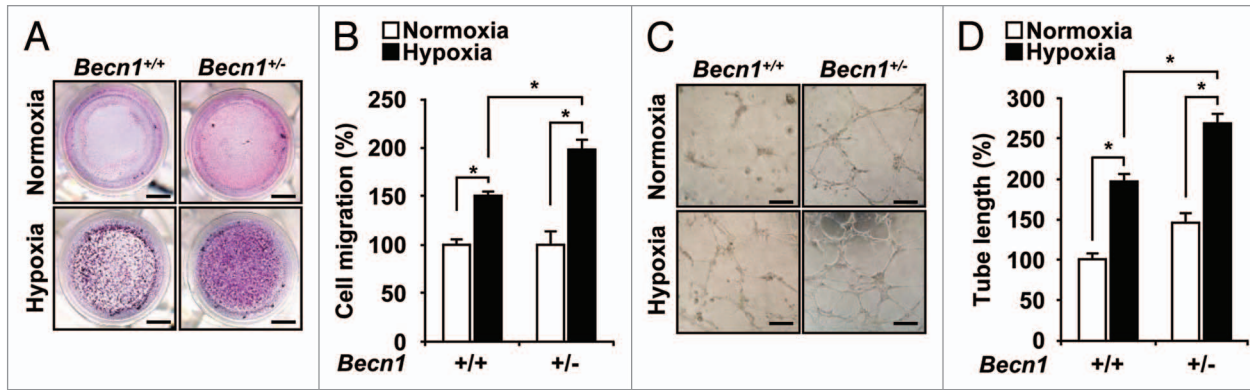


Figure 5. (A) Chemotactic motility of mLECs induced by hypoxia after 12 h of incubation. (Scale bar, 2 mm). (B) Quantification of EC migration through the transwell. Data represent means \pm SEM in triplicate experiments. (* $p < 0.05$, Student's t-test). (C) mLECs were plated on Matrigel-coated wells at a density of 1.8×10^5 cells/well with hypoxia. After 20 h, photomicrographs were taken. (Scale bar, 50 μ m). (D) Graphs show mean capillary-like network on the Matrigel. Images were quantified with ImageJ software. Data are means \pm SEM in triplicate experiments. (* $p < 0.05$, Student's t-test).

evident after 24 h exposure to 5% O_2 , though the magnitude of the response was much weaker (Fig. 8C). The forced expression of Beclin 1 suppressed the hypoxia-dependent increase of HIF-2 α expression in *Becn1*^{+/-} mLECs, but did not affect the expression of

HIF-1 α (Fig. 8D). The differences in HIF-2 α expression between the strains were not attributable to differences in transcriptional regulation. There was no apparent difference in *Hif-2 α* mRNA levels between *Becn1*^{+/-} or *Becn1*^{+/+} mLECs under normoxic or

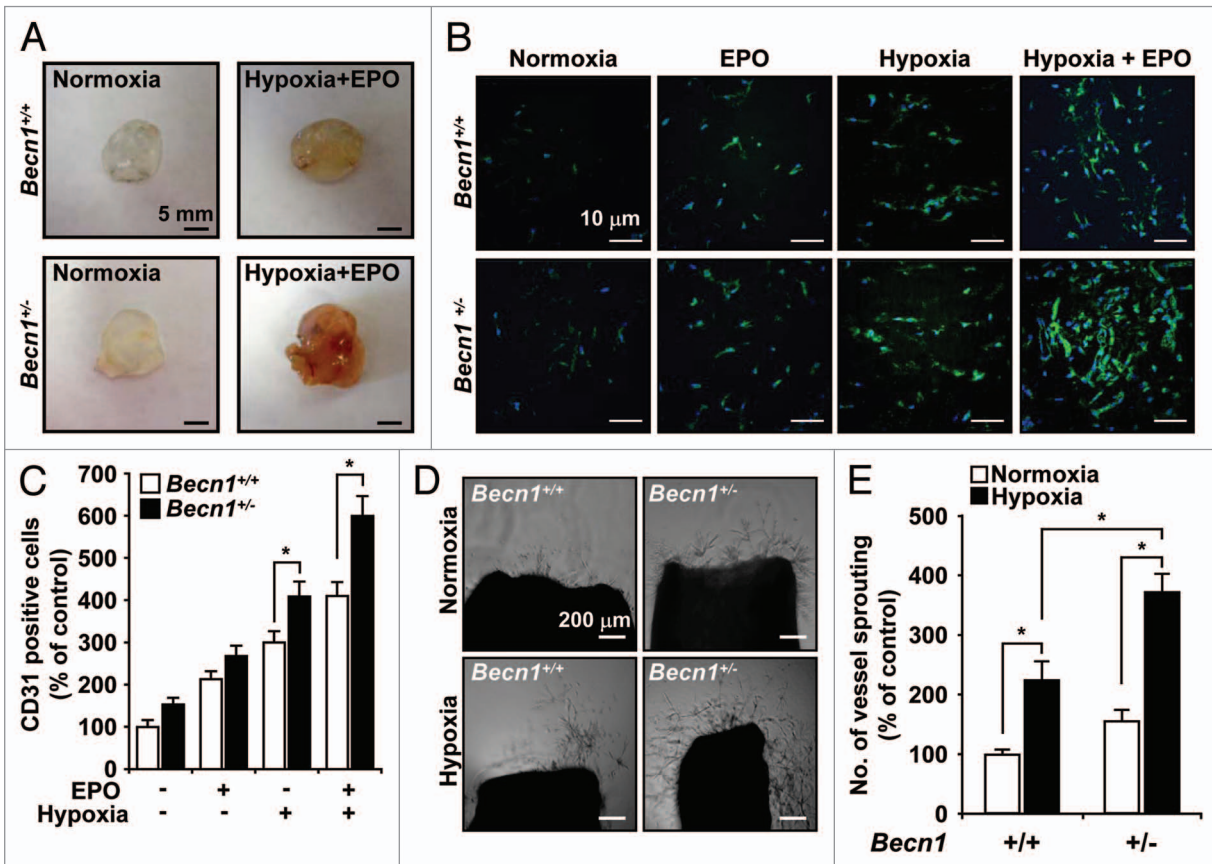


Figure 6. *Becn1*^{+/-} mLEC display increased hypoxia-induced angiogenesis in vivo and vessel sprouting ex vivo. (A) Representative Matrigel plugs were photographed. (B) Plugs were stained for infiltrating ECs using an anti-CD31 antibody. (C) Quantitative assessment of CD31 positive ECs. Data are means \pm SEM (* $p < 0.05$, Student's t-test), $n = 7$ per group. (D) Representative photographs of endothelial cell sprouts formed from the margin of vessel segments. Aortic rings harvested from *Becn1*^{+/+} and *Becn1*^{+/-} were embedded in Matrigel and cultured under normoxia or hypoxia for 10 days. (E) Vessel sprouting was quantified by counting the number of vascular sprouts that directly originated from the mouse aorta. Data are means \pm SEM (* $p < 0.05$, Student's t-test), $n = 8$ per group.

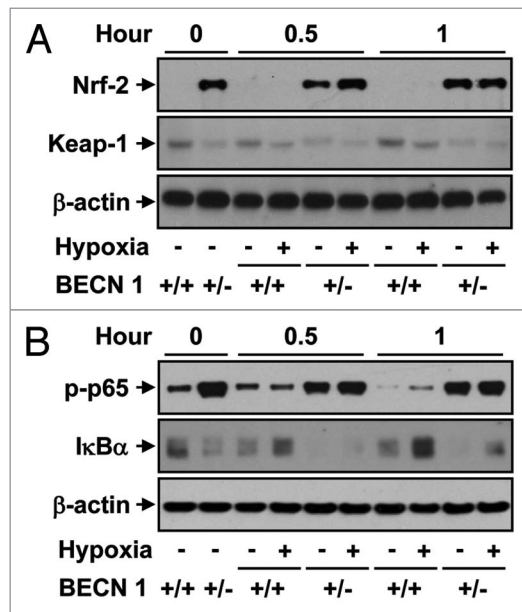


Figure 7. Western blot analysis of (A) Nrf-2 and Keap-1 or (B) phospho (p)-p65 and IκBα levels in *Becn1*^{+/+} and *Becn1*^{+/-} mLEC exposed to hypoxia (1% O₂) for the indicated times. The immunoblot shown is representative of three independent experiments. β-actin served as the standard.

hypoxic conditions (Fig. 8E). In the presence of the translational inhibitor cycloheximide, the half-life of HIF-2α protein during hypoxia exposure was increased in *Becn1*^{+/-} relative to that of *Becn1*^{+/+} mLECs (Fig. 8F).

Enhanced proliferation, migration and tube formation in *Becn1*^{+/-} endothelial cells is dependent on HIF-2α. To determine the functional effects of HIF-1α and HIF-2α in hypoxia-inducible angiogenesis, we transfected *Becn1*^{+/+} and *Becn1*^{+/-} mLECs with *Hif-1α* and *Hif-2α* siRNA (Fig. 9A) and examined their effects on hypoxia-induced proliferation (Fig. 9B), migration (Fig. 9C) and capillary-like tube formation (Fig. 9D). Interestingly *Hif-1α* siRNA inhibited these responses in *Becn1*^{+/+} mLECs whereas *Hif-2α* siRNA preferentially inhibited these responses in *Becn1*^{+/-} mLECs (Fig. 9B–D).

Discussion

Allelic loss of *BECN1* occurs with high frequency in human breast, ovarian and prostate cancers.^{29–32} Enhanced tumorigenesis in *Becn1*^{+/-} mice has been attributed to genomic instability resulting from increased metabolic stress and impaired autophagy.³³ The mechanism by which *Becn1*^{+/-} mice exhibit increased tumorigenesis is not known.²⁹ Using *Becn1*^{+/-} mice and mLECs derived from these mice, we demonstrate that Beclin 1 plays a crucial role in regulating tumorigenesis by suppressing angiogenesis. We observed that hypoxia-induced tumor growth and neovascularization were upregulated in *Becn1*^{+/-} mice compared to *Becn1*^{+/+} mice. Beclin 1 may regulate angiogenic responses by several distinct mechanisms. Although our data demonstrate that Beclin 1 deficiency in mice results in the enhanced production of the circulating factor EPO in vivo, they also implicate a regulatory

role for Beclin 1 in the angiogenic response of endothelial cells. Our results show that *Becn1*^{+/-} mLECs displayed increased angiogenic activity under hypoxia, including capillary formation *ex vivo*, proliferation and endothelial cell migration. Recent studies have reported that endogenous anti-angiogenic molecules such as endostatin and angiostatin, induce autophagy in endothelial cells by modulating Beclin 1 and β-catenin levels.^{34,35} These studies were suggestive of an association of Beclin 1 with the regulation of angiogenesis. Autophagy as a response to hypoxia has also been recently implicated in the regression of hyaloid vessels in early developing retina.³⁶ Here, we conclude that Beclin 1 is associated with the suppression of angiogenesis. However, it remains unclear whether active autophagy is required for the anti-angiogenic effects of Beclin 1, or whether the results reflect a regulatory signaling function of Beclin 1 that is independent of autophagy. The *Becn1*^{+/-} mice displayed reduced autophagosome formation in the lung during hypoxia exposure relative to wild-type mice. Interestingly, the *Becn1*^{+/-} mice also showed reductions in the expression and activation of autophagic protein LC3B in both normoxic and hypoxic conditions. These observations, taken together, suggest that the *Becn1*^{+/-} mice are at least partially compromised in autophagic function. Additional investigation to examine the relationship between autophagic flux and the regulation of angiogenesis may shed further light on this question.

Previous studies have shown that autophagy defects may increase cellular generation of ROS. For example, embryonic fibroblasts derived from *Atg5*-deleted mice have enhanced mitochondrial ROS generation in the context of viral infection.²³ Recently we have shown that macrophages derived from *Becn1*^{+/-} mice exhibit an enhanced production of mitochondrial ROS under basal conditions.²⁴ Furthermore, previous studies have shown that autophagy defects can promote activation of transcription factors (i.e., Nrf-2) and pro-inflammatory regulators such as NFκB.^{25,26} In agreement with these observations, we also find that *Becn1*^{+/-} are primed for pro-inflammatory and stress-related responses, as suggested by elevations in the expressions of Nrf-2 and phospho-p65 (NFκB). Nrf-2 regulated genes (e.g., heme oxygenase-1) as well as NFκB-regulated cytokines can potentially impact angiogenic processes.^{37–39} Thus, the stress-primed phenotype of *Becn1*^{+/-} mice may contribute considerably to the pro-angiogenic balance.

In our study, the differential angiogenic response in *Becn1*^{+/-} mLEC was also associated with a switch from a HIF-1α to HIF-2α dominant phenotype in response to hypoxia. The mechanism for this alteration of the balance of HIF isoforms expression remains unclear. The stabilization of HIF-1α is known to be regulated by reactive oxygen species (ROS) tone.⁴⁰ In light of these observations, the changes in HIF isoform expression evident in *Becn1*^{+/-} mLEC during hypoxic stimulation may be related to differential ROS production and/or pro-inflammatory signaling in endothelial cells and this warrants further investigation.

Although HIF-1α and HIF-2α both heterodimerize with HIF-1β, and recognize the same core element NCGTG in the promoter regions of target genes, these isoforms may regulate distinct transcriptional targets. The factors that govern the specificity and transcriptional activity of these factors with respect

to the regulation of overlapping and non-overlapping gene targets, and the tissue-specificity of these responses remains incompletely clear.²⁷ HIF-2 α is highly expressed in embryonic vascular endothelial cells and activates the expression of target genes whose products modulate vascular function and angiogenesis.^{41,42} HIF-2 α expression has been implicated in the growth and neovascularization of human tumors, including breast and bladder tumors.^{43,44} Mice with targeted endothelial cell-specific deficiency in HIF-2 α developed normally, but displayed increased vessel permeability and aberrant endothelial cell ultrastructure.^{45,46}

Our results indicate specificity for HIF-2 α in the systemic regulation of the pro-angiogenic factor EPO. The *Becn1*^{-/-} mice displayed increased levels of circulating EPO relative to wild-type mice after hypoxic exposure, whereas the levels of VEGF, another major angiogenic factor remained unchanged. In the liver, EPO production is known to be preferentially regulated by HIF-2 α .^{47,48} We cannot exclude the possibility that other pro-angiogenic factors may contribute to the phenotypic observations. Further studies using gene expression or cytokine profiling techniques may uncover additional pro-angiogenic factors that are specifically upregulated in *Becn1*^{-/-} mice.

Interestingly, HIFs have also been shown to regulate the autophagic pathway. HIF-1 α promotes hypoxia-inducible autophagy through activation of the BNIP3 pathway.¹⁵ In contrast, HIF-2 α downregulates autophagy in human and murine cartilage.⁴⁹

Our studies suggest that Beclin 1 status is associated with the regulation of angiogenesis, which is demonstrated here in the presence of hypoxia. However, it should be noted that the tumor growth phenotype of *Becn1*^{-/-} mice also contains a significant normoxic component as shown in Figure 1A, which is not evident in the in vitro assays of angiogenesis and cell proliferation as described in this paper. This normoxic component of tumor growth in *Becn1*^{-/-} mice may be attributed to regulatory effects of Beclin 1 on tumor cell growth that are independent of vascular effects. On the other hand, the regulatory effects of Beclin 1 on

tumor growth during hypoxia stimulation appear to involve elevated stress responses and differential regulation of HIF isoforms in host tissues with consequences on the production of circulating angiogenic factors and the regulation of angiogenesis.

In conclusion, the results of our study are the first to show an association between the autophagic protein Beclin 1 and the regulation of angiogenesis, with implications in tumor

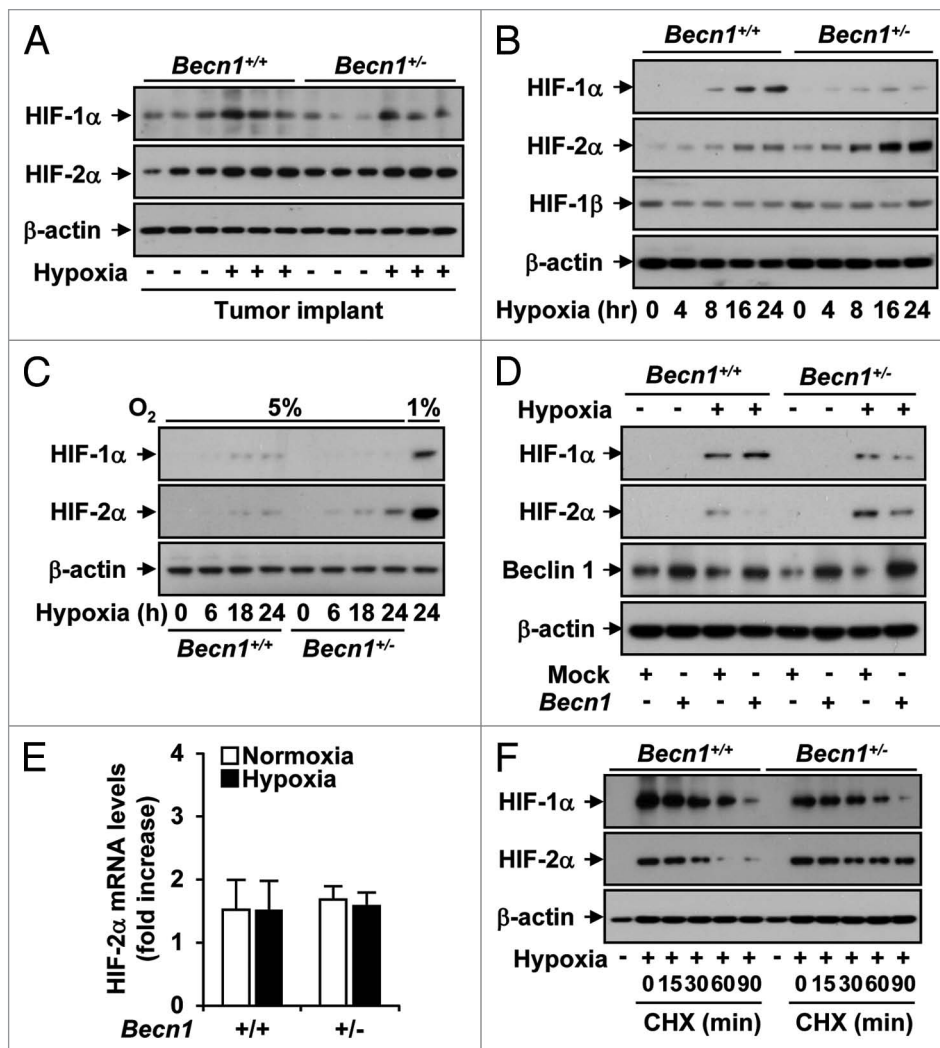


Figure 8. Hypoxia-induced angiogenesis is mediated by a selective increase in HIF-2 α expression in *Becn1*^{-/-} mLECs. (A) Tumor-bearing *Becn1*^{+/+} and *Becn1*^{+/-} mice were subjected to hypoxia or normoxia (3 weeks). Tumor tissue was recovered for analysis of HIF-1 α , HIF-1 β and HIF-2 α levels by western blot analysis. β -actin served as the standard. (B) Western blot analysis of total HIF-1 α , HIF-1 β and HIF-2 α levels in *Becn1*^{+/+} and *Becn1*^{+/-} mLEC exposed to hypoxia (1% O₂) for the indicated times. The immunoblot shown is representative of three independent experiments. β -actin served as the standard. (C) Western blot analysis of total HIF-1 α and HIF-2 α levels in *Becn1*^{+/+} and *Becn1*^{+/-} mLEC exposed to mild hypoxia (5% O₂) for the indicated times. The positive control (lane 9) represents lysate from *Becn1*^{+/+} mLEC exposed to 24 h hypoxia at 1% O₂. β -actin served as the standard. (D) The *Becn1*^{+/+} and *Becn1*^{+/-} mLECs were transfected with Beclin 1 expression vector or vector control (pCMV) and then exposed to hypoxia (1% O₂) or normoxia for 24 h. Western blot analysis was performed to detect the levels of HIF-1 α , HIF-2 α and Beclin 1. The immunoblot shown is representative of three independent experiments. β -actin served as the standard. (E) The *Becn1*^{+/+} and *Becn1*^{+/-} mLECs were subjected to hypoxia (4 h) and analyzed for *Hif-2 α* mRNA levels by qRT-PCR. Data are expressed as fold difference over normoxic wild-type control. (F) The *Becn1*^{+/+} and *Becn1*^{+/-} mLEC were exposed to hypoxia (1% O₂) for 24 hrs followed by treatment with cyclohexamide (CHX) for 0–90 minutes. HIF-1 α and HIF-2 α levels were determined by western immunoblot analysis. β -actin served as the standard.

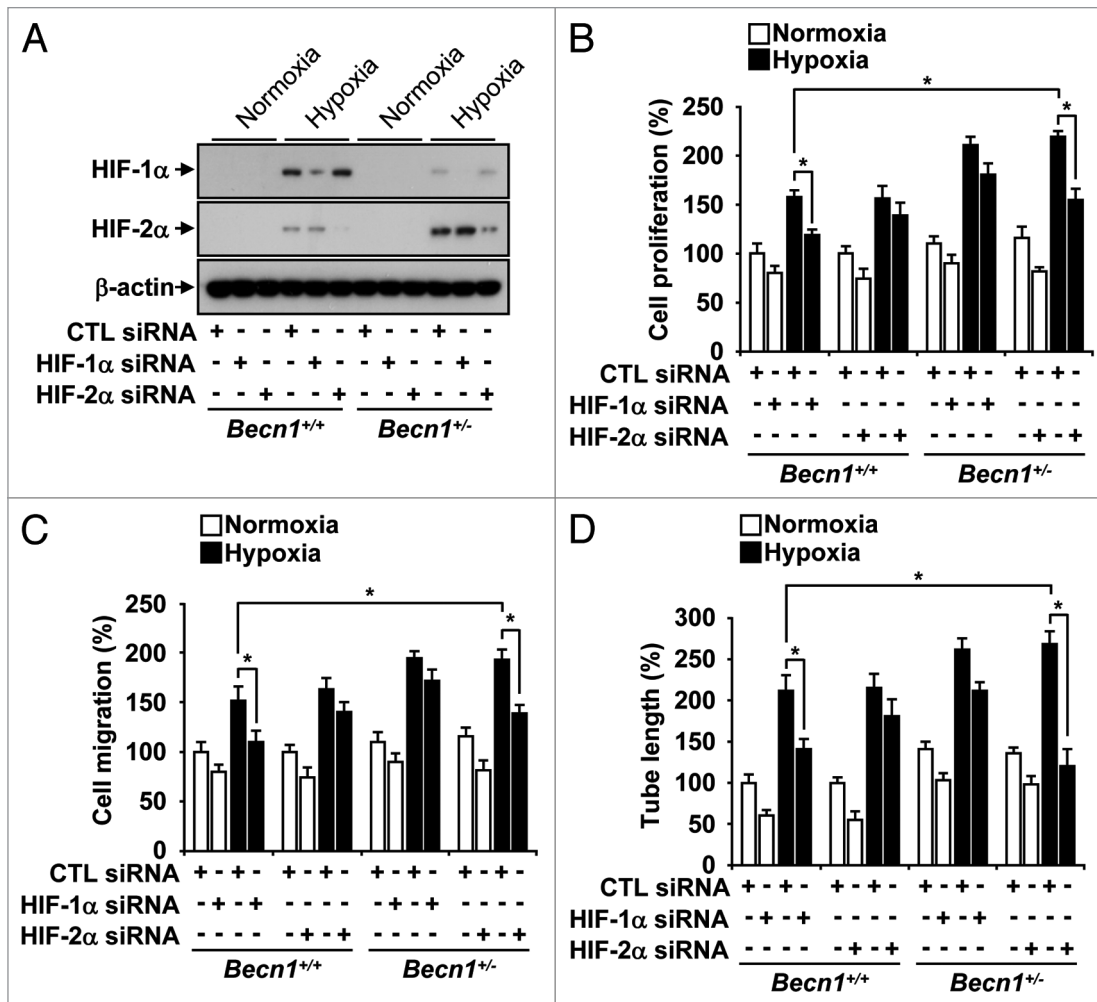


Figure 9. (A) mLEC were infected with siRNA corresponding to *Hif-1α* and *Hif-2α* or control, and then assayed for HIF-1α and HIF-2α protein expression by western immunoblot analysis. β-actin served as the standard. (B–D) *Becln1*^{+/+} and *Becln1*^{+/-} mLEC were infected with siRNA corresponding to *Hif-1α* and *Hif-2α* or control, and then exposed to hypoxia or normoxia. Graphs indicate the quantification of (B) relative cell proliferation (C) migration and (D) tube formation. Data represent means ± SEM from three independent experiments. (*p < 0.05, Student's t-test).

growth and development. We show that *Becln1*^{+/-} vascular cells have elevated indices of stress and pro-inflammatory responses, which could account for in part, the pro-angiogenic phenotype of the corresponding mice. Among these changes, *Becln1*^{+/-} display alterations in HIF-dependent signaling involving differential expression of the α-subunits of HIF. The mechanism(s) by which the expression of HIF-2α is altered in *Becln1*^{+/-} mice remain unclear, but may involve the regulation of protein stability. Further experiments are warranted to determine whether Beclin 1 protein can directly regulate the DNA binding activity of functional HIF-1α/HIF-1β or HIF-2α/HIF-1β heterodimers. The resolution of Beclin 1-dependent anti-angiogenic mechanisms may lead to new treatments for vascular diseases and cancer.

Methods

Chemicals and reagents. We purchased the monoclonal antibody to HIF-1α and HIF-2α from Novus (NB100-134 and

NB100-122), antibodies to HIF-1β and HMB-45 from Abcam (Ab2771 and Ab732), antibodies to Beclin 1 (sc-11427), Nrf-2 (sc-722) and IκBα (sc-371) from Santa Cruz, antibody to β-actin from Sigma (A2228); and the antibody to PECAM from BD Biosciences (557355). Enhanced chemiluminescence reagent was purchased from Thermo Scientific (1859674). All siRNA reagents were purchased from Santa Cruz. Cyclohexamide (C4859), and all other reagents were from Sigma.

Animals and in vivo hypoxia exposure. All animals were housed in accordance with the guidelines from the American Association for Laboratory Animal Care. The Animal Research Committee of Brigham and Women's Hospital approved all protocols. *Becln1*^{+/-} mice (8–12 weeks old) (obtained from B. Levine)¹⁹ and their corresponding age-matched wild-type littermates were placed in a Plexiglas chamber maintained at 10% O₂ (hypoxia group), or in a chamber open to room air (normoxia group) for 3 wks with a 12 h:12 h light-dark cycle. The oxygen concentration in the chamber was verified by an oxygen sensor calibrated for low oxygen tension.

Primary tumor growth. We performed tumor-bearing experiments using B16F10 mouse melanoma cells (American Type Culture Collection, CRL-6475). B16F10 cells were cultured in complete DMEM medium (Invitrogen, 11965) containing 10% FBS (Invitrogen, 10437) and penicillin/streptomycin (Invitrogen, 15140). B16F10 cells were harvested for tumor inoculation by disruption with trypsin/EDTA solution (Invitrogen, 25300), washed with HBSS (Invitrogen, 14175) and centrifuged for 5 min at 400x g. Cells were resuspended in PBS (Invitrogen, 10010) and single subcutaneous injections of 3×10^5 B16F10 cells were administered into the flanks of the mice in a volume of 100 μ l. We exposed the inoculated mice to 10% hypoxia for 3 weeks and monitored tumor growth daily. Primary tumor size was determined by measuring two orthogonal axes with a caliper and tumor weight was determined by the formula: Tumor volume (mm^3) = (width + length)/2 x width x length x 0.5236.⁵⁰ Metastatic lesions were monitored by immunohistochemical staining.

Isolation of mouse lung endothelial cells. Mouse lung endothelial cells (mLECs) were isolated from *Becn1^{+/+}* and *Becn1^{-/-}* mouse lung as previously described in reference 51. Briefly mouse lung was digested in collagenase and filtered through 100 μ m cell strainers, centrifuged and washed twice with medium. Cell suspensions were incubated with a CD31 monoclonal antibody (rat anti-mouse) against platelet endothelial cell adhesion molecule-1 (PECAM) for 30 min at 4°C. The cells were washed twice to remove unbound antibody and resuspended in a binding buffer containing washed magnetic beads coated with sheep anti-rat immunoglobulin G (Invitrogen, 111.35). Attached cells were washed four to five times in culture medium, and then digested with trypsin/EDTA to detach the beads.

Vascular cell culture. Human pulmonary artery endothelial cells (PAEC) were purchased from Lonza (cc-2530). PAEC at passages 5–8 were grown to ~80% confluence in endothelial cell growth medium-2 (EGM-2) supplemented with EGM-2 SingleQuots™ and 2% FBS (Lonza, cc-3162). Human pulmonary artery vascular smooth muscle cells (PASMC) (Lonza, cc-2581) at passages 7–10 were grown to ~80% confluence in smooth muscle cell growth medium-2 (SmGM2) supplemented with SmGM2 SingleQuots™ and 5% FBS (Lonza, cc-3182). The mLEC were cultured in Dulbecco's modified Eagle's medium (DMEM) containing 10% fetal bovine serum (FBS), 6.32 g/liter HEPES (Sigma, H7523) and 16.6 mg/liter of endothelial cell growth supplements (ECGS) (BD Biosciences, 356006). Cells were cultured in humidified incubators at 37°C containing 95% air, 5% CO₂ at 37°C. Cells were grown in 100 mm dishes and detached with 0.05% trypsin, resuspended in complete growth medium and seeded into 35 mm, six-well and 12-well plates for individual experiments. PAECs and mLECs were placed in an airtight Modular Incubator Chamber (Billups-Rothenberg, MIC-101), flushed continuously (10 min) with a premixed gas (1% O₂, 5% CO₂, 94% N₂) (Airgas, NI9422000132) and then incubated for the indicated intervals. Corresponding normoxic controls were maintained for equivalent times in humidified incubators in an atmosphere of 95% air, 5% CO₂.

Western immunoblotting, immunohistochemistry and ELISA. Western immunoblot analyses were performed as

previously described in reference 51. For western blotting, protein concentrations of cell lysates and frozen tissue homogenates were determined using Coomassie plus protein assay (Thermo Fischer Scientific, 1856210) and were resolved by SDS/PAGE using NuPage Novex Bis-Tris 4–12% polyacrylamide gels (Invitrogen, NP0323BOX). Formalin-fixed lung tissue sections were paraffin-embedded for immunohistochemical staining. For ELISA assays, mouse plasma samples were normalized by volume. The levels of VEGF and EPO were determined using the commercially available Quantikine™ kits (R&D Systems) according to the manufacturer's instructions.

Real-time PCR. Total RNA was extracted from cells using TRIZOL reagent (Invitrogen, 5346994) and converted to cDNA using high-capacity cDNA archive kit (Applied Biosystems, 4368814). Quantitative RT-PCR was performed as described in reference 52. Primers for *Hif-2 α* (Mm01236112) and TaqMan Master Mix for gene expression assays (4369016) were purchased from Applied Biosystems. Gene expression was analyzed by the comparative threshold cycle (Ct) method, using GUS- β (Applied Biosystems, Mm03003537) as the internal standards.

Aortic ring sprouting assay. Aortic ring sprouting analyses were performed as previously described in reference 53. Aortas were harvested from 8-week-old *Becn1^{+/+}* and *Becn1^{-/-}* mice and sectioned into several pieces (aortic rings). Cell culture plates (96 well) were coated with 60 μ l Matrigel (BD Biosciences, 354230). After gelling, the rings were placed in the wells and added 40 μ l Matrigel. As a control, aortic rings in endothelial basal medium (EBM) (Lonza, cc-3124) alone and VEGF-containing EBM were assayed. The plates were incubated at 37°C and medium were changed every 2 days for 2 weeks. The angiogenic sprouting from aortic rings was examined in 8 rings per group (N = 5). Each aortic ring was photographed and sprouting was quantified by counting the number of vascular sprouts that directly originated from mouse aorta. We took photomicrographs of individual explants and quantified microvascular sprouting by measuring the area covered by outgrowth of the aortic ring with ImageJ software.

In vivo matrigel plug assay. The Matrigel plug assay was performed as described in reference 54. In brief, 8-week-old *Becn1^{+/+}* and *Becn1^{-/-}* mice were injected subcutaneously with 0.6 ml of Matrigel containing 1 μ g/ml erythropoietin (R&D systems, 959-ME-010) and 10 units of heparin. The injected Matrigel rapidly formed a single, solid gel plug. After 14 days, the skin of the mouse was pulled back to expose the Matrigel plug, which remained intact. To identify infiltrating ECs, immunohistochemistry was performed with anti-CD-31 antibody.

Proliferation, migration and tube formation. Cell proliferation was determined by the 3-(4,5-Dimethylthiazol-2-yl)-2,5-diphenyl tetrazolium bromide (MTT) assay (Sigma, M5655). Cell counts were performed using a hemocytometer and viable cells were visualized with Trypan blue (Invitrogen, 15250). Migration assays were performed as previously described in reference 53. Briefly, the chemotactic motility of *Becn1^{+/+}* and *Becn1^{-/-}* mLECs was assayed using Transwell plates (VWR, 29442-120) with 6.5 mm-diameter polycarbonate filters (8 μ m pore size). The lower surface of the filter was coated with 10 μ g of gelatin.

Fresh DMEM containing 15% FBS and ECGSs were placed in the lower wells. Both mLECs were trypsinized and suspended at a final concentration of 1×10^6 cells/ml in DMEM containing 1% FBS. The chamber was incubated with 1% hypoxia at 37°C for 8 h. After incubation, the cells were fixed and stained with hematoxylin and eosin. Nonmigrating cells were mechanically removed from the upper surface of the filter and migration was observed using an inverted microscope. Images were captured with digital camera and cells were quantified by counting the cells that migrated to the lower side. The formation of tube-like structures by mLECs on growth factor-reduced Matrigel was performed as previously described in reference 53. Tissue culture plates (24 well) were coated with Matrigel according to the manufacturer's instructions. The cells were plated onto the layer of Matrigel at a density of 2.0×10^5 cells/well, and then exposed to room air or hypoxia. After 20 h, imaging of tube formation was performed on an Axiovert-25 inverted microscope equipped with a digital camera (Carl Zeiss) and the area covered by the tube network was quantified using ImageJ software (National Institutes of Health).

Small interfering RNA and overexpression. Human PAEC or mLEC were transiently transfected with human *BECN1* siRNA (Santa Cruz, sc-29797) or mouse *Becn1* siRNA (Santa Cruz, sc-29798), mouse *Hif-1 α* siRNA (Santa Cruz, sc-35562), mouse *Hif-2 α* siRNA (Santa Cruz, sc-35317) respectively, or control-siRNA (Santa Cruz, sc-108060) as directed by the manufacturer. PAEC at passages 6–8 were seeded at 5×10^4 cells per well in 12-well dishes. After 24 h each well was approximately 80–90% confluent. The media was changed to transfection media (Santa Cruz, sc-108062) for 2 h. 10 nM siRNA was incubated with transfection reagent (Santa Cruz, sc-108061) for 1 h and then added to each well. After 4–6 h, the media was aspirated and complete media replaced in each well.

References

- Risau W. Mechanisms of angiogenesis. *Nature* 1997; 386:671-4.
- Folkman J. Angiogenesis in cancer, vascular, rheumatoid and other disease. *Nat Med* 1995; 1:27-31.
- Pouyssegur J, Dayan F, Mazure NM. Hypoxia signaling in cancer and approaches to enforce tumor regression. *Nature* 2006; 25:437-43.
- Tennant DA, Duran RV, Boulahbel H, Gottlieb E. Metabolic transformation in cancer. *Carcinogenesis* 2009; 30:1269-80.
- Semenza GL. Vascular responses to hypoxia and ischemia. *Arterioscler Thromb Vasc Biol* 2010; 30:648-52.
- Semenza GL. Defining the role of hypoxia-inducible factor 1 in cancer biology and therapeutics. *Oncogene* 2010; 29:625-34.
- Shweiki D, Itin A, Soffer D, Keshet E. Vascular endothelial growth factor induced by hypoxia may mediate hypoxia-initiated angiogenesis. *Nature* 1992; 359:843-45.
- Pugh CW, Ratcliffe PJ. Regulation of angiogenesis by hypoxia: role of the HIF system. *Nat Med* 2003; 9:677-84.
- Janmaat ML, Heerkens JL, de Bruin AM, Klous A, de Waard V, de Vries CJ. Erythropoietin accelerates smooth muscle cell-rich vascular lesion formation in mice through endothelial cell activation involving enhanced PDGF-BB release. *Blood* 2010; 115:1453-60.
- Grimm C, Wenzel A, Groszer M, Mayser H, Seeliger M, Samardzija M, et al. HIF-1-induced erythropoietin in the hypoxic retina protects against light-induced retinal degeneration. *Nat Med* 2002; 8:718-24.
- Tian H, McKnight SL, Russell DW. Endothelial PAS domain protein 1 (EPAS1), a transcription factor selectively expressed in endothelial cells. *Genes Dev* 1997; 11:72-82.
- Imamura T, Kikuchi H, Herraiz MT, Park DY, Mizukami Y, Mino-Kenduson M, et al. HIF-1 α and HIF-2 α have divergent roles in colon cancer. *Int J Cancer* 2009; 124:763-71.
- Deberardinis RJ, Lum JJ, Hatzivassiliou G, Thompson CB. The biology of cancer: metabolic reprogramming fuels cell growth and proliferation. *Cell Metab* 2008; 7:11-20.
- Rankin EB, Giaccia AJ. The role of hypoxia-inducible factors in tumorigenesis. *Cell Death Differ* 2008; 15:678-85.
- Zhang H, Bosch-Marce M, Shimoda LA, Tan YS, Baek JH, Wesley JB, et al. Mitochondrial autophagy is an HIF-1-dependent adaptive metabolic response to hypoxia. *J Biol Chem* 2008; 283:10892-903.
- Yorimitsu T, Klionsky DJ. Autophagy: molecular machinery for self-eating. *Cell Death Differ* 2005; 12:1542-52.
- Mizushima N, Levine B, Cuervo AM, Klionsky DJ. Autophagy fights disease through cellular self-digestion. *Nature* 2008; 451:1069-75.
- Liang XH, Kleeman LK, Jiang HH, Gordon G, Goldman JE, Berry G, et al. Protection against fatal Sindbis virus encephalitis by beclin, a novel Bcl-2-interacting protein. *J Virol* 1998; 72:8586-96.
- Liang XH, Jackson S, Seaman M, Brown K, Kempkes B, Hibshoosh H, et al. Induction of autophagy and inhibition of tumorigenesis by beclin 1. *Nature* 1999; 402:672-6.
- Itakura E, Kishi C, Inoue K, Mizushima N. Beclin 1 forms two distinct phosphatidylinositol-3-kinase complexes with mammalian Atg14 and UVRAG. *Mol Biol Cell* 2008; 19:5360-72.
- Itakura E, Mizushima N. Atg14 and UVRAG: mutually exclusive subunits of mammalian Beclin 1-P13K complexes. *Autophagy* 2009; 5:534-6.
- Zhong Y, Wang QJ, Li X, Yan Y, Backer JM, Chait BT, et al. Distinct regulation of autophagic activity by Atg14L and Rubicon associated with Beclin 1-phosphatidylinositol-3-kinase complex. *Nat Cell Biol* 2009; 11:468-76.
- Tal MC, Sasai M, Lee HK, Yordy B, Shadel GS, Iwasaki A. Absence of autophagy results in reactive oxygen species-dependent amplification of RLR signaling. *Proc Natl Acad Sci USA* 2009; 106:2770-5.
- Nakahira K, Haspel JA, Rathinam VA, Lee SJ, Dolinay T, Lam HC, et al. Autophagy proteins regulate innate immune responses by inhibiting the release of mitochondrial DNA mediated by the NALP3 inflammasome. *Nat Immunol* 2011; 12:222-30.

Electron microscopy and imaging. For electron microscopy, tissue sections were fixed in 2.5% glutaraldehyde in PBS after experimental manipulations. These tissues were photographed using a JEOL JEM 1210 transmission electron microscope (JEOL) at 80 or 60 kV onto electron microscope film (ESTAR thick base; Kodak) and printed onto photographic paper. For microscopy, lung tissue sections were fixed in formalin and embedded in paraffin. Imaging of tube formation, migration and HMB45 immunofluorescence was performed on an Axiovert-25 inverted microscope equipped with a digital camera (Carl Zeiss). Confocal imaging of CD31 (PECAM) which is endothelial marker was performed on an LSM510 meta inverted microscope equipped with an oil immersion lens at 40x objective, with a confocal laser scanning head (Carl Zeiss). Digital images were acquired for analysis (SPOT, Diagnostic Instruments, Inc.).

Statistical analyses. Data are presented as mean plus or minus SD. Statistical comparisons between groups were performed by the use of one-way analysis of variance followed by the Student t-test.

Acknowledgements

We thank Dr. Beth Levine (University of Texas) for the *Becn1*^{+/−} mice and Emeka Ifedigbo for animal handling. This work was supported by NIH grants R01-HL60234, R01-HL55330, R01-HL079904 and a FAMRI Clinical Innovator Award to A.M.K. Choi. S. Ryter was supported by NIH grants (R01-HL60234, R01-HL079904) and received salary support from the Lovelace Respiratory Research Institute.

25. Lau A, Wang XJ, Zhao F, Villeneuve NF, Wu T, Jiang T, et al. A noncanonical mechanism of Nrf2 activation by autophagy deficiency: direct interaction between Keap1 and p62. *Mol Cell Biol* 2010; 30:3275-85.
26. Kim HP, Wang X, Chen ZH, Lee SJ, Huang MH, Wang Y, et al. Autophagic proteins regulate cigarette smoke-induced apoptosis: protective role of heme oxygenase-1. *Autophagy* 2008; 4:887-95.
27. Mole DR, Blancher C, Copley RR, Pollard PJ, Gleadle JM, Ragoussis J, et al. Genome-wide association of hypoxia-inducible factor (HIF)-1 α and HIF-2 α DNA binding with expression profiling of hypoxia-inducible transcripts. *J Biol Chem* 2009; 284:16767-75.
28. Hu CJ, Wang LY, Chodosh LA, Keith B, Simon MC. Differential roles of hypoxia-inducible factor 1 α (HIF-1 α) and HIF-2 α in hypoxic gene regulation. *Mol Cell Biol* 2003; 23:9361-74.
29. Qu X, Yu J, Bhagat G, Furuya N, Hibshoosh H, Troxel A, et al. Promotion of tumorigenesis by heterozygous disruption of the beclin 1 autophagy gene. *J Clin Invest* 2003; 112:1809-20.
30. Eccles DM, Russell SE, Haites NE, Atkinson R, Bell DW, Gruber L, et al. Early loss of heterozygosity on 17q in ovarian cancer. *Oncogene* 1992; 7:2069-72.
31. Futreal PA, Söderkvist P, Marks JR, Iglehart JD, Cochran C, Barrett JC, et al. Detection of frequent allelic loss on proximal chromosome 17q in sporadic breast carcinoma using microsatellite. *Cancer Res* 1992; 52:2624-7.
32. Gao X, Zacharek A, Salkowski A, Grignon DJ, Sakr W, Porter AT, et al. Loss of heterozygosity of the BRCA1 and other loci on chromosome 17q in human prostate cancer. *Cancer Res* 1995; 55:1002-5.
33. Karantza-Wadsworth V, Patel S, Kravchuk O, Chen G, Mathew R, Jin S, et al. Autophagy mitigates metabolic stress and genome damage in mammary tumorigenesis. *Genes Dev* 2007; 21:1621-35.
34. Nguyen T, Subramanian IV, Xiao X, Ghosh G, Nguyen P, Kelekar A, et al. Endostatin induces autophagy in endothelial cells by modulating beclin 1 and β -catenin levels. *J Cell Mol Med* 2009; 13:3687-98.
35. Nguyen TM, Subramanian IV, Kelekar A, Ramakrishnan S. Kringle 5 of human plasminogen, an angiogenesis inhibitor, induces both autophagy and apoptotic death in endothelial cells. *Blood* 2007; 109:4793-802.
36. Kim JH, Kim JH, Yu YS, Mun JY, Kim KW. Autophagy-induced regression of hyaloid vessels in early ocular development. *Autophagy* 2010; 6:922-8.
37. Bussolati B, Mason JC. Dual role of VEGF-induced heme-oxygenase-1 in angiogenesis. *Antioxid Redox Signal* 2006; 8:1153-63.
38. Mantovani A. Molecular pathways linking inflammation and cancer. *Curr Mol Med* 2010; 10:369-73.
39. Kim TH, Hur EG, Kang SJ, Kim JA, Thapa D, Lee YM, et al. NRF2 blockade suppresses colon tumor angiogenesis by inhibiting hypoxia-induced activation of HIF-1 α . *Cancer Res* 2011; 71:2260-75.
40. Chandel NS, McClintock DS, Feliciano CE, Wood TM, Melendez JA, Rodriguez AM, Schumacker PT. Reactive oxygen species generated at mitochondrial complex III stabilize hypoxia-inducible factor-1 α during hypoxia: a mechanism of O₂ sensing. *J Biol Chem* 2000; 275:25130-8.
41. Licht AH, Muller-Holtkamp F, Flamme I, Breier G. Inhibition of hypoxia-inducible factor activity in endothelial cells disrupts embryonic cardiovascular development. *Blood* 2006; 107:584-90.
42. Skuli N, Liu L, Runge A, Wang T, Yuan L, Patel S, et al. Endothelial deletion of hypoxia-inducible factor-2 α (HIF-2 α) alters vascular function and tumor angiogenesis. *Blood* 2007; 114:469-77.
43. Leek RD, Talks KL, Pezzella F, Turley H, Campo L, Brown NS, et al. Relation of hypoxia-inducible factor-2 α (HIF-2 α) expression in tumor-infiltrative macrophages to tumor angiogenesis and the oxidative thymidine phosphorylase pathway in Human breast cancer. *Cancer Res* 2002; 62:1326-9.
44. Onita T, Ji PG, Xuan JW, Sakai H, Kanetake H, Maxwell PH, et al. Hypoxia-induced, perinecrotic expression of endothelial Per-ARNT-Sim domain protein-1/hypoxia-inducible factor-2 α correlates with tumor progression, vascularization and focal macrophage infiltration in bladder cancer. *Clin Cancer Res* 2002; 8:471-80.
45. Gordan JD, Hu CJ, Diehl JA, Simon MC. HIF-2 α promotes hypoxic cell proliferation by enhancing c-myc transcriptional activity. *Cancer Cell* 2007; 11:335-47.
46. Higgins DF, Kimura K, Iwano M, Haase VH. Hypoxia-inducible factor signaling in the development of tissue fibrosis. *Cell Cycle* 2008; 7:1128-32.
47. Rankin EB, Biju MP, Liu Q, Unger TL, Rha J, Johnson RS, et al. Hypoxia-inducible factor-2 (HIF-2) regulates hepatic erythropoietin in vivo. *J Clin Invest* 2007; 117:1068-77.
48. Kapitsinou PP, Liu Q, Unger TL, Rha J, Davidoff O, Keith B, et al. Hepatic HIF-2 regulates erythropoietic responses to hypoxia in renal anemia. *Blood* 2010; 116:3039-48.
49. Bohensky J, Terkhorn SP, Freeman TA, Adams CS, Garcia JA, Shapiro IM, et al. Regulation of autophagy in human and murine cartilage: hypoxia-inducible factor 2 suppresses chondrocyte autophagy. *Arthritis Rheum* 2009; 60:1406-15.
50. Bandyopadhyay S, Zhan R, Chaudhuri A, Watabe M, Pai SK, Hirota S, et al. Interaction of KAI1 on tumor cells with DARC on vascular endothelium leads to metastasis suppression. *Nat Med* 2006; 12:933-8.
51. Wang X, Zhou Y, Kim HP, Song R, Zarnegar R, Ryter SW, et al. Hepatocyte growth factor protects against hypoxia/reoxygenation-induced apoptosis in endothelial cells. *J Biol Chem* 2004; 279:5237-43.
52. Lee SJ, Smith A, Guo L, Alastalo TP, Li M, Sawada H, et al. Autophagic protein LC3B confers resistance against hypoxia-induced pulmonary hypertension. *Am J Respir Crit Care Med* 2010; [Epub ahead of print].
53. Lee SJ, Namkoong S, Kim YM, Kim CK, Lee H, Ha KS, et al. Fractalkine stimulates angiogenesis by activating the Raf-1/MEK/ERK- and PI3K/Akt/eNOS-dependent signal pathways. *Am J Physiol Heart Circ Physiol* 2006; 291:2836-46.
54. Choi YS, Choi HJ, Min JK, Pyun BJ, Maeng YS, Park H, et al. Interleukin-33 induces angiogenesis and vascular permeability through ST2/TRAF6-mediated endothelial nitric oxide production. *Blood* 2009; 114:3117-26.